Dynamics of an A-DNA homopolymer crystal with sodium ions: A Green-function approach

L. Chern and E. W. Prohofsky
Department of Physics, Purdue University, West Lafayette, Indiana 47907
(Received 11 September 1992)

We apply lattice dynamics to calculate the vibrational modes of a perfect A-DNA homopolymer crystal with sodium ions. A Green-function method is used to reduce the dimension of the matrix to be diagonalized. We concentrate on the biologically significant crystal modes with frequencies less than 100 wave numbers. 94% of the crystal modes were likely to be located in this frequency range. Characteristics of the crystal modes are analyzed. We find that the interhelical modes dominate in the frequency range 25–30 cm^{-1} and the intrahelical modes dominate for frequencies greater than 80 cm^{-1}. The infrared absorption peaks at 35, 50, and 83 cm^{-1} in our model. The former two bands are not counterion dependent and the latter one is. Our Raman scattering spectrum peaks around 30 cm^{-1} and it is strongly counterion dependent. The counterion-dependency trend of this band is the same as that of the experimental 25-cm^{-1} feature, extrapolated to 0 relative humidity, observed in both DNA and RNA crystals. The characteristics of the experimental Raman scattering features at 25 and 35 cm^{-1} are consistent with our results.

PACS number(s): 87.10.+e, 87.15.−v

I. INTRODUCTION

The normal modes of a symmetric isolated double helical molecule were originally studied by Eyster and Prohofsky [1]. The whole double helix was then modeled as a one-dimensional solid and the lattice dynamics of the system was studied. Young, Prabhu, and Pohofsky studied the dynamics of an isolated DNA molecule with counterions and a water envelope [2]. The force constants associated with chemical bonds used in the calculation were obtained by fitting the theoretical results to the observed Raman scattering lines above 400 cm^{-1} [3]. The model for nonbonded force constants was developed for electrostatic interactions between charged atoms. These calculations were successful in reproducing the general features of the Raman spectra for the optical modes near $\mathbf{k}$(wave vector)$=\mathbf{0}$. Young, Prabhu, and Prohofsky [2] modeled a coupling between two helices which included counterions and water molecules, attempting to predict the interhelical modes. The limited agreement of that work has stimulated this more thorough attempt to model the crystal form. The principal reason to study crystalline DNA is the finding that the spectra should be sharper than that for fibers. The best experimental data should come from the best crystals even though the isolated helix modes are used exclusively in theoretical studies. One needs to be able to separate out effects due to crystal effects.

A DNA crystal is treated as an infinite three-dimensional lattice with the smallest repetitive combination of DNA segments as the unit cell. The size of the DNA crystal unit cell varies. According to Lindsay [4], a crystal unit cell has, at the minimum, two to three 360° turns of separate helices. Including the external groups of atoms such as sodium ions and water molecules, the minimum number of atoms per crystal cell is approximately 1000. It is very clumsy to carry out the study of the dynamics of the DNA crystal in a straightforward way without utilizing the facilities of a supercomputer such as a Cray Model YMP/8. Solutions by this method require diagonalization of a matrix of dimension (3000×3000). To reduce the size of the problem we turn to the Green-function method to determine the normal modes of a DNA crystal. It has the further advantage that the interhelical modes are found as combinations of the biologically more significant helix modes.

The Green-function method provides us with a means to obtain exact solutions for the lattice dynamics of lattices with defects based on the solutions for the dynamics of perfect lattices. The normal modes of a DNA crystal without the interhelical interactions are determined first. All of these modes can be found from our single-helix solutions of the homopolymer DNA molecule which only require diagonalization of a (129×129) matrix. This system can be taken as a solid made up of isolated helices. The interactions between atoms belonging to the same DNA molecule are called the "intrahelical interactions" and those between atoms belonging to different DNA molecules are the "interhelical interactions." We will treat the interhelical interactions as the "defect" from the system of noninteracting helices.

Use of the Green function can reduce the size of the problem to the size of the force matrix of the defects which is much smaller because the "defects" involve only a few atoms. We approximate the interhelical interactions by considering only the interactions between some nearby atoms of adjacent DNA molecules. The smaller the number of atoms chosen to involve in the interhelical interactions, the more use of the Green function can reduce the dimension of the problem but the less accurate the approximation of the true interhelical crystal is. With careful choice of atoms for the interhelical interactions, we reduce the size of the matrix to be diagonalized from (2858×2858) to (264×264).

The assumptions made for this calculation are as follows. (a) Similar to the case of an isolated DNA mole-

cule, the hydrogen atoms are assigned to either the carbon, oxygen, or nitrogen atoms to which the hydrogen atoms attach. This measure enables us to reduce the degrees of freedom of the problem by a large amount without distorting the essence of the dynamics of the DNA molecules. (b) Each phosphate group in the DNA crystal is assigned a sodium ion and the position of the sodium ion is assumed to be on the diagonal axis of the parallelogram formed by the phosphorus and the two free oxygen atoms of the phosphate group. (c) The set of force constants between the atoms of the same double helix in the DNA crystal was adopted from the force fields used to calculate the vibrational modes of an isolated DNA molecule [2]. This set of refined force constants has given results in good agreement with experimental observations [2]. (d) The interhelical interactions are assumed to be the summations of the van der Waals and electrostatic interactions between the sodium ions, phosphorus atoms, and the two free oxygen atoms of the phosphate groups of adjacent double helices since these atoms are at the outer rim of DNA molecules. The effect due to water clusters is not considered in this study.

Coordinates

A-DNA forms a monoclinic crystal that can be generated by fundamental translation vectors, $a=21.7$ Å, $b=39.9$ Å, and $c=28.0$ Å. The angles between the translation vectors are $\alpha=\angle(b,c)=90.0°$, $\gamma=\angle(a,b)=90.0°$, and $\beta=\angle(a,c)=96.8°$ [5]. Each crystal unit cell contains two 360° double helical turns which belong to two separate double helices. There are 22 base pairs in each crystal unit cell. The two DNA turns lie parallel to the **c** axis. Each 360° turn segment is named "a segment." The two segments are located at (0,0,0) and $(\frac{1}{2},\frac{1}{2},0)$. Pitch and pitch angle of the *A*-GC segments are, respectively, 2.548 Å and 32.7° (G denotes guanine and C cytosine).

Various observations have shown that Na^+ ions do not appear to be localized in either DNA fibers or crystals [5]. However, fitted ion positions are required in order to carry out this calculation. Simulations by Clementi and Corongiu [6] indicate that the sodium ions, strongly attracted to the free phosphate oxygen atoms, follow helical patterns along the backbones. The average distance from the sodium ion to the two free oxygen atoms of the phosphate group was calculated to be 2.7 Å [2,7]. After we consider the short-range electrostatic force between the ions and the phosphate atoms and the atomic and ionic radii of the atoms, the final positions for Na^+ were chosen to be on the diagonal axis of the O(1)—P—O(2) parallelogram and the distance from Na^+ to the nearby O(1), O(2) and the phosphorous atoms is, respectively 2.67, 2.67, and 3.14 Å. One sodium ion is assigned to each phosphate group. The charge of each sodium ion is assumed to be 1.00 in units of electron charge. Including the ions, there are 43 atoms, excluding the hydrogen atoms, in each base pair. The degrees of freedom of this DNA homopolymer crystal is 2838.

II. DYNAMICS OF A DNA CRYSTAL

The dynamics of an isolated DNA molecule has been fully studied by Prohofsky and co-workers [1–3,8–10]. The dynamics of a DNA crystal is an extension of that of an isolated DNA molecule. Numerous notations are used to label the dynamics of DNA at different levels to avoid confusion. Table I lists the labels and the corresponding levels of the dynamics of DNA.

Kinetic energy of a DNA crystal can be expressed in the mass-weighted Cartesian (MWC) coordinates

$$2T=\sum_{\mathbf{n}=-\infty}^{\infty}\dot{\Xi}_{\mathbf{n}}^{\dagger}\dot{\Xi}_{\mathbf{n}},\quad \infty\equiv(\infty,\infty,\infty)\ . \tag{1}$$

The $\mathbf{n}=(n_a,n_b,n_c)$ is the index vector for the crystal unit cells. $\Xi_{\mathbf{n}}$ is the MWC coordinate vector of the **n**th crystal unit cell. The MWC coordinate for atom i is defined as

$$\xi i=\frac{\mathbf{q}_i}{\sqrt{m_i}}\ , \tag{2}$$

with $\mathbf{q}_i$ and m_i being the Cartesian displacement vector and mass of the atom i.

We express the MWC coordinates in terms of the MWC symmetry coordinates, $X(\Theta)$,

$$\Xi_{\mathbf{n}}=(2\pi)^{-3/2}\int_{-\pi}^{\pi}\int_{-\pi}^{\pi}\int_{-\pi}^{\pi}X(\Theta)\exp(-i\mathbf{n}\cdot\Theta)d^3\Theta\ . \tag{3}$$

$\Theta=(\Theta_a,\Theta_b,\Theta_c)$ is the phase difference vector between crystal unit cells. Wave vector $\mathbf{k}=(k_a,k_b,k_c)$ is

$$k_a=\Theta_a/21.7\text{ Å},\quad k_b=\Theta_b/39.9\text{ Å},\quad k_c=\Theta_a/28.0\text{ Å}\ . \tag{4}$$

The Fourier expansion of the δ function in three dimensions is

$$\delta(\Theta-\Theta')=\frac{1}{(2\pi)^3}\sum_{\mathbf{n}=-\infty}^{\infty}\exp[-i\mathbf{n}\cdot(\Theta-\Theta')]\ . \tag{5}$$

Kinetic energy of the DNA crystal can be shown to be

$$2T=\int_{-\pi}^{\pi}\int_{-\pi}^{\pi}\int_{-\pi}^{\pi}\dot{X}^{\dagger}(\Theta)\dot{X}(\Theta)d^3\Theta\ . \tag{6}$$

We assume that the force between each pair of atoms is harmonic, therefore we can write the potential energy of the DNA crystal as

$$2V=\sum_{\mathbf{n}=-\infty}^{\infty}\sum_{\mathbf{m}=(0,0,0)}^{\infty}Q_{\mathbf{n},\mathbf{n}+\mathbf{m}}^{T}F^{\mathbf{m}}Q_{\mathbf{n},\mathbf{n}+\mathbf{m}}\ . \tag{7}$$

$Q_{\mathbf{n},\mathbf{n}+\mathbf{m}}$ is the redundant internal coordinate vector be-

TABLE I. Labels for different levels of the DNA dynamics.

Label	Dynamics of DNA
b	DNA molecule with one base pair as a unit cell
s	DNA molecule with one segment (360° turn) as a unit cell
cr	DNA crystal with both the interhelical and intrahelical interactions
inter	DNA crystal with only the interhelical interactions
intra	DNA crystal with only the intrahelical interactions

tween nth and (n+m)th crystal unit cells. $F^{\mathbf{m}}$ is the force constant matrix and it only depends on the separation of the two crystal unit cells. In a valence-force-field analysis [11] there are four types of internal coordinates; i.e., bond stretch, angle bend, torsion, and bond bending out of a plane [2,11]. The nonbonded forces are generally treated as stretches between the pairs of atoms involved in electrostatic interactions [2]. The interhelical interactions are the summation of all of the nonbonded stretches between atoms of different double helices.

We use matrix D to link the internal coordinates to the MWC coordinates. For $\mathbf{m}=(0,0,0)$, the internal coordinates are within the same crystal unit cell. We can express the internal coordinates within the nth unit cell as

$$Q_{\mathbf{n},\mathbf{n}}=D_{\mathbf{0},\mathbf{0}}\Xi_{\mathbf{n}} . \tag{8}$$

$D_{\alpha,\beta}$ gives the expansion coefficients of the internal coordinates between two crystal unit cells separated by β units to the MWC coordinates of the two unit cells. α indicates the unit cells at the two ends of the internal coordinates and it can be either $\mathbf{0}$ or β. See Fig. 1.

For $\mathbf{m}\neq(0,0,0)$, the internal coordinates between unit cells $\mathbf{n}$ and $\mathbf{n}+\mathbf{m}$ are

$$Q_{\mathbf{n},\mathbf{n}+\mathbf{m}}=D_{\mathbf{0},\mathbf{m}}\Xi_{\mathbf{n}}+D_{\mathbf{m},\mathbf{m}}\Xi_{\mathbf{n}+\mathbf{m}} . \tag{9}$$

Potential energy then becomes

$$2V=\sum_{\mathbf{n}=-\infty}^{\infty}\left\{(D_{\mathbf{0},\mathbf{0}}\Xi_{\mathbf{n}})^{T}F^{\mathbf{0}}(D_{\mathbf{0},\mathbf{0}}\Xi_{\mathbf{n}})+\sum_{\mathbf{m}\,(\neq\mathbf{0})}^{\infty}[(D_{\mathbf{0},\mathbf{m}}\Xi_{\mathbf{n}}+D_{\mathbf{m},\mathbf{m}}\Xi_{\mathbf{n}+\mathbf{m}})^{T}\times F^{\mathbf{m}}(D_{\mathbf{0},\mathbf{m}}\Xi_{\mathbf{n}}+D_{\mathbf{m},\mathbf{m}}\Xi_{\mathbf{n}+\mathbf{m}})]\right\} \tag{10}$$

$$=\int_{-\pi}^{\pi}\int_{-\pi}^{\pi}\int_{-\pi}^{\pi}X^{\dagger}(\Theta)M_{\mathrm{cr}}(\Theta)X(\Theta)d^{3}\Theta . \tag{11}$$

$M_{\mathrm{cr}}(\Theta)$ is the M matrix for the DNA crystal and it incorporates the force constant matrix F and the transformation matrix D,

$$M_{\mathrm{cr}}(\Theta)=D_{\mathbf{0},\mathbf{0}}^{T}F^{\mathbf{0}}D_{\mathbf{0},\mathbf{0}}+\sum_{\mathbf{m}\,(\neq\mathbf{0})}^{\infty}[D_{\mathbf{0},\mathbf{m}}^{T}F^{\mathbf{m}}D_{\mathbf{0},\mathbf{m}}+e^{i\mathbf{m}\cdot\Theta}D_{\mathbf{m},\mathbf{m}}^{T}F^{\mathbf{m}}D_{\mathbf{0},\mathbf{m}}+e^{-i\mathbf{m}\cdot\Theta}D_{\mathbf{0},\mathbf{m}}^{T}F^{\mathbf{m}}D_{\mathbf{m},\mathbf{m}}+D_{\mathbf{m},\mathbf{m}}^{T}F^{\mathbf{m}}D_{\mathbf{m},\mathbf{m}}] . \tag{12}$$

With both the kinetic energy and potential energy in the MWC symmetry coordinates, we have the equation of motion for the DNA crystal

$$\ddot{X}(\Theta)+M_{\mathrm{cr}}(\Theta)X(\Theta)=0 . \tag{13}$$

Let $X(\Theta)=R(\Theta)e^{-i\omega t}$ and we have

$$[M_{\mathrm{cr}}(\Theta)-\omega^{2}I]R(\Theta)=0 . \tag{14}$$

ω is the oscillation frequency for the DNA crystal. To obtain a nontrivial solution of $X(\Theta)$, we let

$$\det[M_{\mathrm{cr}}(\Theta)-\omega^{2}I]=0 . \tag{15}$$

If $S_{\mathrm{cr}}(\Theta)$ and $\Lambda_{\mathrm{cr}}(\Theta)$ are, respectively, the eigenvector and eigenvalue of matrix $M_{\mathrm{cr}}(\Theta)$, we have

$$[M_{\mathrm{cr}}(\Theta)S_{\mathrm{cr}}(\Theta)-S_{\mathrm{cr}}(\Theta)\Lambda_{\mathrm{cr}}(\Theta)]=0 . \tag{16}$$

cr indicates that the matrices are for the DNA crystal with both the interhelical and intrahelical interactions.

We divide the potential energy such that

$$V=V_{\mathrm{intra}}+V_{\mathrm{inter}} , \tag{17}$$

$$2V_{\mathrm{intra}}=\sum_{\mathbf{n}=-\infty}^{\infty}\sum_{\mathbf{m}=\mathbf{0}}^{\infty}Q_{\mathbf{n},\mathbf{n}+\mathbf{m}}^{T}F_{\mathrm{intra}}^{\mathbf{m}}Q_{\mathbf{n},\mathbf{n}+\mathbf{m}} , \tag{18}$$

$$2V_{\mathrm{inter}}=\sum_{\mathbf{n}=-\infty}^{\infty}\sum_{\mathbf{m}=\mathbf{0}}^{\mathbf{m}=\infty}Q_{\mathbf{n},\mathbf{n}+\mathbf{m}}^{T}F_{\mathrm{inter}}^{\mathbf{m}}Q_{\mathbf{n},\mathbf{n}+\mathbf{m}} . \tag{19}$$

F_{intra} and F_{inter} contain force constants for the intrahelical and interhelical interactions. Without the interhelical interactions, only the atoms belonging to the same DNA double helix have interactions with each other, therefore $\mathbf{m}\|\mathbf{c}$. It can be shown that the potential energy of the DNA crystal due to only the intrahelical interactions is

$$2V_{\mathrm{intra}}=\int_{-\pi}^{\pi}\int_{-\pi}^{\pi}\int_{-\pi}^{\pi}X^{\dagger}(\Theta)M_{\mathrm{intra}}(\Theta_{c})X(\Theta)d^{3}\Theta , \tag{20}$$

where

$$M_{\mathrm{intra}}(\Theta_{c})=D_{\mathbf{0},\mathbf{0}}^{T}F_{\mathrm{intra}}^{\mathbf{m}}D_{\mathbf{0},\mathbf{0}}+\sum_{\mathbf{m}=m_{c}\hat{c},m_{c}=1}^{m_{c}=\infty}[D_{\mathbf{0},\mathbf{m}}^{T}F_{\mathrm{intra}}^{\mathbf{m}}D_{\mathbf{0},\mathbf{m}}+e^{im\Theta_{c}}D_{\mathbf{m},\mathbf{m}}^{T}F_{\mathrm{intra}}^{\mathbf{m}}D_{\mathbf{0},\mathbf{m}}+e^{-im\Theta_{c}}D_{\mathbf{0},\mathbf{m}}F_{\mathrm{intra}}^{\mathbf{m}}D_{\mathbf{m},\mathbf{m}}+D_{\mathbf{m},\mathbf{m}}^{T}F_{\mathrm{intra}}^{\mathbf{m}}D_{\mathbf{m},\mathbf{m}}] . \tag{21}$$

Since there are no interhelical interactions involved, the oscillation wave can only propagate along the helix axis and the phase difference vectors only exist in the c direction. The explicit matrix forms are

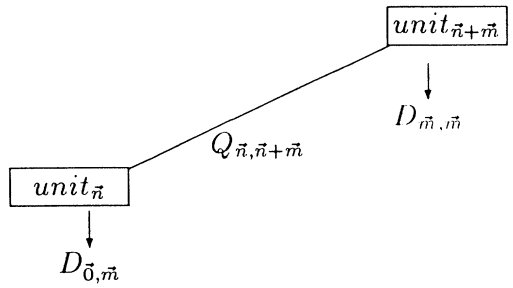

FIG. 1. D matrix for DNA crystals. The internal coordinates between unit $\mathbf{n}$ and $\mathbf{n}+\mathbf{m}$ are $Q_{\mathbf{n},\mathbf{n}+\mathbf{m}}=D_{\mathbf{0},\mathbf{m}}\Xi_{\mathbf{n}}+D_{\mathbf{m},\mathbf{m}}\Xi_{\mathbf{n}+\mathbf{m}}$.

$$M_{\text{intra}}(\Theta)=\begin{bmatrix} M_s(\Theta_c) & 0 \\ 0 & M_s(\Theta_c) \end{bmatrix} . \tag{22}$$

$$S_{\text{intra}}(\Theta)=\begin{bmatrix} S_s(\Theta_c) & 0 \\ 0 & S_s(\Theta_c) \end{bmatrix} , \tag{23}$$

and

$$\Lambda_{\text{intra}}(\Theta)=\begin{bmatrix} \Lambda_s(\Theta_c) & 0 \\ 0 & \Lambda_s(\Theta_c) \end{bmatrix} . \tag{24}$$

M_s, S_s, and Λ_s are for an isolated DNA molecule with one segment as a unit cell and they are discussed in Appendix A.

There are interhelical interactions not only between the two segments of the same crystal unit cell, I and II, but also between the nearby segments of neighboring crystal unit cells, mainly in the directions (1,0,0), (0,1,0), and (1,1,0). Thus V_{inter} can be approximated as

$$\begin{aligned} 2V_{\text{inter}} &= \sum_{\mathbf{n}=-\infty}^{\infty} [\, Q^T_{\mathbf{n},\mathbf{n}} F^{000}_{\text{inter}} Q_{\mathbf{n},\mathbf{n}} + Q^T_{\mathbf{n},\mathbf{n}+(1,0,0)} F^{100}_{\text{inter}} Q_{\mathbf{n},\mathbf{n}+(1,0,0)} \\ &\quad + Q^T_{\mathbf{n},\mathbf{n}+(0,1,0)} F^{010}_{\text{inter}} Q_{\mathbf{n},\mathbf{n}+(0,1,0)} + Q^T_{\mathbf{n},\mathbf{n}+(1,1,0)} F^{110}_{\text{inter}} Q_{\mathbf{n},\mathbf{n}+(1,1,0)} \,] \qquad (25) \\ &= \int_{-\pi}^{\pi}\int_{-\pi}^{\pi}\int_{-\pi}^{\pi} X^{\dagger}(\Theta) M_{\text{inter}}(\Theta_a,\Theta_b) X(\Theta) d^3\Theta , \qquad (26) \end{aligned}$$

$$\begin{aligned} M_{\text{inter}}(\Theta_a,\Theta_b) &= D^T_{00} F^0_{\text{I,II}} D_{00} + D^T_{0,100} F^{100} D_{0,100} + e^{i\Theta_a} D^T_{100,100} F^{100} D_{0,100} \\ &\quad + e^{-i\Theta_a} D^T_{0,100} F^{100} D_{100,100} + D^T_{100,100} F^{100} D_{100,100} + D^T_{0,010} F^{010} D_{0,010} \\ &\quad + e^{i\Theta_b} D^T_{010,010} F^{010} D_{0,010} + e^{-i\Theta_b} D^T_{0,010} F^{010} D_{010,010} + D^T_{010,010} F^{010} D_{010,010} \\ &\quad + D^T_{0,110} F^{110} D_{0,110} + e^{i(\Theta_a+\Theta_b)} D^T_{110,110} F^{110} D_{0,110} \\ &\quad + e^{-i(\Theta_a+\Theta_b)} D^T_{0,110} F^{110} D_{110,110} + D^T_{110,110} F^{110} D_{110,110} . \end{aligned} \tag{27}$$

The equation of motion becomes

$$[M_{\text{intra}}(\Theta_c)+M_{\text{inter}}(\Theta_a,\Theta_b)-w^2 I] R(\Theta)=0 . \tag{28}$$

M_{inter} will be treated as the "defect" from M_{intra}.

Let $X_j(\delta)$ represent the jth eigenvector of $M_{\text{cr}}(\delta)$. This mode is degenerate with $X_j(-\delta)=X_j^*(\delta)$ for $\delta\neq 0$ [1]. They are transformed into one another by the time-reversal operator. Similar to the dynamics of an isolated DNA molecule, we can construct an orthogonal pair such as

$$\begin{aligned} X^a_j(\delta) &= \frac{1}{\sqrt{2}}[X_j(\delta)+X_j(-\delta)] , \\ X^b_j(\delta) &= \frac{1}{\sqrt{2}i}[X_j(\delta)-X_j(-\delta)] . \end{aligned} \tag{29}$$

Let $\Xi_{\mathbf{m}j}$ represent the actual Cartesian displacements of the atoms in the $\mathbf{m}$th unit cell during the jth normal mode of phase difference δ and frequency w_j. We have

$$\xi^a_{\mathbf{m}j}=\frac{\pi^{-3/2}}{\sqrt{2}}\text{Re}[X_j(\delta)e^{-i\mathbf{m}\cdot\delta}] , \tag{30}$$

$$\xi^b_{\mathbf{m}j}=\frac{\pi^{-3/2}}{\sqrt{2}}\text{Im}[X_j(\delta)e^{-i\mathbf{m}\cdot\delta}] . \tag{31}$$

For the modes at zone center, $\delta=\mathbf{0}$, the displacement vector X_j is real and we have

$$\xi_{\mathbf{m}j}=(2\pi)^{-3/2}[X_j(\mathbf{0})] . \tag{32}$$

III. GREEN-FUNCTION APPROACH

As mentioned, the equations of motion of a DNA crystal without the interhelical interactions are [12]

$$[M_{\text{intra}}(\Theta_c)-w^2 I] R(\Theta_c)=0 , \tag{33}$$

and

$$[M_{\text{intra}}(\Theta_c) S_{\text{intra}}(\Theta_c)-S_{\text{intra}}(\Theta_c)\Lambda_{\text{intra}}(\Theta_c)]=0 , \tag{34}$$

with $M_{\text{intra}}(\Theta_c)$, $S_{\text{intra}}(\Theta_c)$, and $\Lambda_{\text{intra}}(\Theta_c)$ defined in Eqs. (22)–(24).

We define the Green function G as

$$G(M_{\text{intra}}(\Theta_c)-\lambda I)=I . \tag{35}$$

The Green function is a function of Θ_c and λ. It is mentioned in Appendix A that S_s satisfies the unitary condition, therefore so does $S_{\text{intra}}(\Theta_c)$; i.e., $S^{\dagger}_{\text{intra}}(\Theta_c) S_{\text{intra}}(\Theta_c)=I$. From Eq. (34), we have

$$S^{\dagger}_{\text{intra}} M_{\text{intra}} S_{\text{intra}}=\Lambda_{\text{intra}} . \tag{36}$$

Multiply $S^{\dagger}_{\text{intra}}$ and S_{intra} to the left- and right-hand sides

of Eq. (35) and we get

$$S^{\dagger}_{\text{intra}} G S_{\text{intra}} [S^{\dagger}_{\text{intra}} M_{\text{intra}} S_{\text{intra}} - \lambda I] = I \ . \tag{37}$$

Plug in Eq. (36) and we have

$$S^{\dagger}_{\text{intra}} G S_{\text{intra}} [\Lambda_{\text{intra}} - \lambda I] = I \ . \tag{38}$$

Let $\Delta \equiv \Lambda_{\text{intra}}(\Theta_c) - \lambda I$ and it becomes

$$S^{\dagger}_{\text{intra}} G S_{\text{intra}} \Delta = I \ . \tag{39}$$

Δ is a diagonal matrix. Let

$$K = \Delta^{-1} = \begin{bmatrix} K_{\text{I}}(\Theta_c) & 0 \\ 0 & K_{\text{II}}(\Theta_c) \end{bmatrix} , \tag{40}$$

then

$$G = S_{\text{intra}} K S^{\dagger}_{\text{intra}} \ , \tag{41}$$

$$G = \begin{bmatrix} S_{s,\text{I}} K_{\text{I}} S^{\dagger}_{s,\text{I}} & 0 \\ 0 & S_{s,\text{II}} K_{\text{II}} S^{\dagger}_{s,\text{II}} \end{bmatrix} = \begin{bmatrix} G_{\text{I}} & 0 \\ 0 & G_{\text{II}} \end{bmatrix} . \tag{42}$$

$K_{\text{I}} = K_{\text{II}}$ and their elements are $K_{x,ij}(\Theta_c) = (\lambda_{ix} - \lambda)^{-1} \delta_{ij}$. λ_{ix} is the ith eigenvalue of DNA segment x, x =I or II and i =1 to 129.

Apply the Green function to the equation of motion of a DNA crystal and let $H \equiv M_{\text{inter}}$ and $\lambda \equiv w^2$. We obtain the new equation of motion

$$[I + GH(\Theta_a, \Theta_b)] R(\Theta) = 0 \ . \tag{43}$$

To obtain a nontrivial solution of $R(\Theta)$, we have

$$\det[I + G(\Theta_c, \lambda) H(\Theta_a, \Theta_b)] = 0 \ . \tag{44}$$

The total interhelical interaction is taken to be the summation of all of the interactions between all of the POOI groups. POOI is the short name for the phosphorus and the two free oxygen atoms of a phosphate group and the ion next to the phosphate group. We arrange the MWC coordinates of the crystal unit cell so that the coordinates of all of the POOI atoms in each segment follow those of the rest of the atoms in that segment.

$$\Xi_{\mathbf{n}} = \begin{bmatrix} \hat{\Xi}^{\text{I}}_{\mathbf{n}} \\ \tilde{\Xi}^{\text{I}}_{\mathbf{n}} \\ \hat{\Xi}^{\text{II}}_{\mathbf{n}} \\ \tilde{\Xi}^{\text{II}}_{\mathbf{n}} \end{bmatrix} . \tag{45}$$

$\tilde{\Xi}^{x}_{\mathbf{n}}(264 \times 1)$ are the MWC coordinates for the POOI atoms in segment x, x =I or II, of crystal unit cell $\mathbf{n}$ and $\hat{\Xi}^{x}_{\mathbf{n}}(1155 \times 1)$ are those for the rest of the atoms in segment x. The matrix of force constants due to the interhelical interactions then has the form

$$H = \begin{bmatrix} 0 & 0 & 0 & 0 \\ 0 & H_{\text{I,I}} & 0 & H_{\text{I,II}} \\ 0 & 0 & 0 & 0 \\ 0 & H^{T}_{\text{I,II}} & 0 & H_{\text{II,II}} \end{bmatrix} . \tag{46}$$

All the elements in the matrix are zero except for those of POOI atoms.

Similar to the MWC coordinates, we arrange $S_{s,x}(\Theta_c)$ such that

$$S_{s,x}(\Theta_c) = \begin{bmatrix} \hat{S}_{s,x}(\Theta_c) \\ \tilde{S}_{s,x}(\Theta_c) \end{bmatrix} , \quad x = \text{I or II} \ . \tag{47}$$

$\tilde{S}_{s,x}(\Theta_c)$ are the part of the displacement vector for the POOI atoms in segment x and $\hat{S}_{s,x}(\Theta_c)$ that for the rest of the atoms in that segment. One part of the Green function then becomes

$$G_{\text{I}} = \begin{bmatrix} G^{11}_{\text{I}} & G^{12}_{\text{I}} \\ G^{12T}_{\text{I}} & G^{22}_{\text{I}} \end{bmatrix} , \tag{48}$$

where $G^{11}_{\text{I}} = \hat{S}_{s,\text{I}} K_{\text{I}} \hat{S}^{\dagger}_{s,\text{I}}$, $G^{12}_{\text{I}} = \hat{S}_{s,\text{I}} K_{\text{I}} \tilde{S}^{\dagger}_{s,\text{I}}$, and $G^{22}_{\text{I}} = \tilde{S}_{s,\text{I}} K_{\text{I}} \tilde{S}^{\dagger}_{s,\text{I}}$. The equation of motion therefore has the form

$$\begin{bmatrix} \hat{R}_{\text{I}} \\ \tilde{R}_{\text{I}} \\ \hat{R}_{\text{II}} \\ \tilde{R}_{\text{II}} \end{bmatrix} = - \begin{bmatrix} 0 & G^{12}_{\text{I}} H_{\text{I,I}} & 0 & G^{12}_{\text{I}} H_{\text{I,II}} \\ 0 & G^{22}_{\text{I}} H_{\text{I,I}} & 0 & G^{22}_{\text{I}} H_{\text{I,II}} \\ 0 & G^{12}_{\text{II}} H^{T}_{\text{I,II}} & 0 & G^{12}_{\text{II}} H_{\text{II,II}} \\ 0 & G^{22}_{\text{II}} H^{T}_{\text{I,II}} & 0 & G^{22}_{\text{II}} H_{\text{II,II}} \end{bmatrix} \begin{bmatrix} \hat{R}_{\text{I}} \\ \tilde{R}_{\text{I}} \\ \hat{R}_{\text{II}} \\ \tilde{R}_{\text{II}} \end{bmatrix} . \tag{49}$$

This equation relates the motion of all the atoms in the crystal unit cell in terms of those involved in the interhelical interactions, POOI. We solve the motion for POOI atoms from the homogeneous equations

$$\begin{bmatrix} \tilde{R}_{\text{I}} \\ \tilde{R}_{\text{II}} \end{bmatrix} = - \begin{bmatrix} G^{22}_{\text{I}} H_{\text{I,I}} & G^{22}_{\text{I}} H_{\text{I,II}} \\ G^{22}_{\text{II}} H^{T}_{\text{I,II}} & G^{22}_{\text{II}} H_{\text{II,II}} \end{bmatrix} \begin{bmatrix} \tilde{R}_{\text{I}} \\ \tilde{R}_{\text{II}} \end{bmatrix} . \tag{50}$$

The condition for nontrivial solution is

$$\det \left[I + \begin{bmatrix} G^{22}_{\text{I}} H_{\text{I,I}} & G^{22}_{\text{I}} H_{\text{I,II}} \\ G^{22}_{\text{II}} H^{T}_{\text{I,II}} & G^{22}_{\text{II}} H_{\text{II,II}} \end{bmatrix} \right] = 0 \ , \tag{51}$$

or

$$\det[I + G' H'] = 0 \ . \tag{52}$$

where

$$G' = \begin{bmatrix} G^{22}_{\text{I}} & 0 \\ 0 & G^{22}_{\text{II}} \end{bmatrix} \text{ and } H' = \begin{bmatrix} H_{\text{I,I}} & H_{\text{I,II}} \\ H^{T}_{\text{I,II}} & H_{\text{II,II}} \end{bmatrix} . \tag{53}$$

Because of the symmetry of the two DNA segments in the crystal unit cell, we can further reduce the dimension of the problem. Since the two segments of the crystal unit cell are identical, we have $K_{\text{I}} = K_{\text{II}}$ and $S_{s,\text{I}} = S_{s,\text{II}}$, therefore $G_{\text{I}} = G_{\text{II}}$, $H_{\text{I,I}} = H_{\text{II,II}}$, and $H_{\text{I,I}} = H^{T}_{\text{I,I}}$. H' has symmetric form

$$H' = \begin{bmatrix} H_a & H_b \\ H_b & H_a \end{bmatrix} . \tag{54}$$

$H_a = H_{\text{I,I}}$ and $H_b = H_{\text{I,II}}$ are both Hermitian matrices; i.e., $H_a = H^{T}_a$ and $H_b = H^{T}_b$.

The equation of motion for POOI atoms can be simplified to become

$$\begin{bmatrix} A & B \\ B & A \end{bmatrix} \begin{bmatrix} \tilde{R}_{\mathrm{I}} \\ \tilde{R}_{\mathrm{II}} \end{bmatrix} = 0 \ , \tag{55}$$

where $A = I + G_{\mathrm{I}}^{22} H_{\mathrm{I,I}} = I + \tilde{S}_{s,\mathrm{I}} K_{\mathrm{I}} \tilde{S}_{s,\mathrm{I}}^{\dagger} H_a$ and $B = G_{\mathrm{I}}^{22} H_{\mathrm{I,II}} = \tilde{S}_{s,\mathrm{I}} K_{\mathrm{I}} \tilde{S}_{s,\mathrm{I}}^{\dagger} H_b$.

In order to obtain the nontrivial solutions, either $\det(A+B)$ or $\det(A-B)$ should be 0. If $\det(A+B)=0$, then $\tilde{R}_{\mathrm{I}} = \tilde{R}_{\mathrm{II}}$, thus $R_{\mathrm{I}} = R_{\mathrm{II}}$. These modes will be referred to as the "in-phase" crystal modes. In these modes, all of the DNA molecules in the crystal move in the same manner. If $\det(A-B)=0$, then $\tilde{R}_{\mathrm{I}} = -\tilde{R}_{\mathrm{II}}$, thus $R_{\mathrm{I}} = -R_{\mathrm{II}}$. These modes will be called the "antiphase" crystal modes. All of the adjacent DNA molecules move in the opposite directions.

Conclusively, we solve equations

$$\det[I + \tilde{S}_{s,\mathrm{I}} K_{\mathrm{I}} \tilde{S}_{s,\mathrm{I}}^{\dagger} (H_a + H_b)] = 0 \tag{56}$$

for in-phase crystal modes and

$$\det[I + \tilde{S}_{s,\mathrm{I}} K_{\mathrm{I}} \tilde{S}_{s,\mathrm{I}}^{\dagger} (H_a - H_b)] = 0 \tag{57}$$

for antiphase crystal modes. The dimension of both equations is (264×264).

The parts of the displacement vector for the rest of the atoms in the crystal unit become

$$\hat{R}_{\mathrm{I}} = \hat{R}_{\mathrm{II}} = -G_{\mathrm{I}}^{12} (H_a + H_b) \tilde{R}_{\mathrm{I}} \tag{58}$$

for in-phase modes and

$$\hat{R}_{\mathrm{I}} = -\hat{R}_{\mathrm{II}} = -G_{\mathrm{I}}^{12} (H_a - H_b) \tilde{R}_{\mathrm{I}} \tag{59}$$

for antiphase modes.

Coefficient of crystal modes in terms of segment modes

It is helpful to express the crystal modes in terms of the crystal modes without the interhelical interactions. The following linear transformation is used [1]:

$$R = S_{\mathrm{intra}} C \ . \tag{60}$$

Elements of vector C are the expansion coefficients of the crystal mode R in terms of S_{intra}. C is found by multiplying both sides of the equation by $S_{\mathrm{intra}}^{\dagger}$. With the unitary condition, $S_{\mathrm{intra}}^{\dagger} S_{\mathrm{intra}} = I$, we have

$$C = S_{\mathrm{intra}}^{\dagger} R = -S_{\mathrm{intra}}^{\dagger} G H R = -K S_{\mathrm{intra}}^{\dagger} H' R \ , \tag{61}$$

therefore

$$C = -\begin{bmatrix} K_{\mathrm{I}} & 0 \\ 0 & K_{\mathrm{II}} \end{bmatrix} \begin{bmatrix} \tilde{S}_{s,\mathrm{I}}^{\dagger} & 0 \\ 0 & \tilde{S}_{s,\mathrm{II}}^{\dagger} \end{bmatrix} \begin{bmatrix} H_a & H_b \\ H_b & H_a \end{bmatrix} \begin{bmatrix} \tilde{R}_{\mathrm{I}} \\ \tilde{R}_{\mathrm{II}} \end{bmatrix} . \tag{62}$$

For in-phase modes, $\tilde{R}_{\mathrm{I}} = \tilde{R}_{\mathrm{II}} = s$, we have

$$C = \begin{bmatrix} c \\ c \end{bmatrix} , \tag{63}$$

where $c = -K_{\mathrm{I}} \tilde{S}_{s,\mathrm{I}}^{\dagger} (H_a + H_b) s$. For antiphase modes, $\tilde{R}_{\mathrm{I}} = -\tilde{R}_{\mathrm{II}} = s$,

$$C = \begin{bmatrix} c \\ -c \end{bmatrix} , \tag{64}$$

where $c = -K_{\mathrm{I}} \tilde{S}_{s,\mathrm{I}}^{\dagger} (H_a - H_b) s$.

IV. RESULT

A. Crystal modes

It is difficult to solve for λ analytically due to the large dimension of the equations and the constraints of computer capability. We therefore solved λ numerically.

Only the crystal modes at the zone center ($\mathbf{k}=\mathbf{0}$ or $\Theta_a = \Theta_b = \Theta_c = 0$) were calculated as these are the only crystal modes that cause Raman scattering and infrared absorption. We targeted the final crystal modes at frequency less than 100 cm^{-1} since this range of frequency was suspected of being involved in the important physical characteristics of DNA such as the helix softening and melting. The frequency shifts from the segment modes to the crystal modes are small as the frequency approaches 100 cm^{-1}. We expect 422 crystal modes in this frequency range. There should be 211 of both in-phase and antiphase crystal modes. In reality, 198 in-phase modes and 199 anti-phase modes are found. They count as 94% of the total expected crystal modes in this frequency region.

53% of the crystal modes fall in frequency range 20–45 cm^{-1}, and the crystal mode density is the largest in the range 25–30 cm^{-1}.

B. Low-frequency crystal modes

We have four zero-frequency modes for an isolated DNA molecule; i.e., one torsional and one longitudinal mode and two transverse bending modes [13]. These four zero-frequency modes either reappear or combine with each other into new modes with higher frequency in the DNA crystal.

Since there are 946 (N) atoms in each crystal unit cell, we have three acoustic branches and 2835 ($3N-3$) optical branches in the dispersion curve of the DNA crystal. There are three zero-frequency translational modes at zone center and they are all in-phase modes. The directions of motion for these degenerate modes are, respectively, (0.69,0.72,0.0), (−0.78,0.62,0.0), and (0,0,1) in the frame of the three translational vectors **a**, **b**, and **c**. Since they are degenerate, in reality, the displacement is a blend of the three translational motions.

Next to the three zero-frequency modes in the in-phase branch, a low-frequency mode at 8.66 cm^{-1} follows, where all of the DNA molecules in the crystal twist along their own crystal axis in the same phase. This mode has zero frequency for an isolated DNA molecule. The interhelical interactions cause this mode to undergo a very large frequency shift.

As to the antiphase modes, at 6.0 cm^{-1} DNA atoms propagate mainly on the plane perpendicular to the helix axis with a small mixture of translational motion along the helix axis. This is the lowest-lying optical mode for this DNA crystal. At 6.5 cm^{-1}, DNA molecules move parallel to the helix axis where if one DNA molecule goes up along the helix axis, then all of the adjacent DNA molecules go down. Again, the interhelical interactions cause this mode to undergo a very large frequency shift. The frequency shift for the torsional motion appears to

be larger than that of translational motion along the helix axis. At frequency 7.96 cm^{-1}, neighboring DNA molecules twist along their own helix axis in the opposite directions. At 8.54 cm^{-1}, DNA molecules mainly twist along the helix axis with a small combination of translational motion on the plane perpendicular to the axis.

C. Interhelical and intrahelical modes

According to the degree of the effect of the interhelical interactions, the DNA crystal modes are roughly classified into two categories; i.e., the "interhelical modes" and the "intrahelical modes." The intrahelical modes are the crystal modes which do not undergo a big change due to the introduction of the interhelical interactions and they reflect the characteristics of the internal bonding between the atoms of the same double helix. These modes can be detected for the DNA either in solution or crystal form. The interhelical modes are the DNA modes which experience a significant effect from the interhelical interactions and these modes do not exist in an isolated DNA molecule. These modes can only be detected in the DNA of crystal form.

The crystal modes which come directly from corresponding segment modes are the intrahelical modes since the introduction of the interhelical interactions does not alter the displacement pattern of these modes. The atom displacement vectors are preserved while their frequencies change due to the crystal field effects, whereas the crystal modes which come from more than one segment mode are the interhelical modes because these modes did not exist until the interhelical interactions were introduced. The interhelical interactions cause some segment modes with different frequencies to combine into a new crystal mode with a new frequency. These modes reflect the characteristics of the crystal packing. If the position of the DNA molecules in the lattice is changed, we expect large changes in characteristics of these interhelical modes. The details of the distribution of interhelical and intrahelical modes in different frequency ranges are summarized in Table II.

There are 140 and 255 intrahelical and interhelical modes which account for 35% and 65% of the total crystal modes in this frequency range. The total number of the interhelical modes is about two times that of the intrahelical modes. 64% of the interhelical modes fall in the 20–45-cm^{-1} region with 20–25 cm^{-1} being the area where the mode density is the largest. The intrahelical modes spread out and, generally speaking, there are more intrahelical modes in high-frequency regions than there are in the low-frequency regions. In the 20–30-cm^{-1} region there are no intrahelical modes. Along with the fact that there are a significant number of interhelical modes in this area, we expect the 20–30-cm^{-1} region to be very strongly interhelical mode in nature as the strength of the interhelical interactions coupled with the mass of the helices tends to bring about resonances in the region. For the area of frequency greater than 80 cm^{-1} intrahelical modes dominate the interhelical ones, therefore this area must be intrahelical-mode oriented.

In short, we found that the interhelical modes dominate in the frequency range 25–30 cm^{-1} and the intrahelical modes dominate in the area of frequency greater than 80 cm^{-1}.

It was observed in experiment [14] that the crystal modes within frequency range 30–35 cm^{-1} are mostly in-

TABLE II. Distribution of the interhelical and intrahelical modes, number of modes, and fraction of total number of modes. $\mathcal{A}$ is the fraction of the crystal modes that are intrahelical while $\mathcal{B}$ is the fraction that are interhelical for each range.

	Crystal modes	Intrahelical modes		Interhelical modes	
Range (cm^{-1})	No.	No. (%)	$\mathcal{A}$ (%)	No. (%)	$\mathcal{B}$ (%)
0–5	3	3 (2.1)	100.0	0 (0.0)	0.0
5–10	5	2 (1.4)	40.0	3 (1.2)	60.0
10–15	0	0 (0.0)		0 (0.0)	
15–20	11	6 (4.3)	54.5	5 (2.0)	45.5
20–25	27	0 (0.0)	0.0	27 (10.6)	100.0
25–30	68	0 (0.0)	0.0	68 (26.7)	100.0
30–35	44	8 (5.7)	18.2	36 (14.1)	81.8
35–40	36	5 (3.6)	13.9	31 (12.2)	86.1
40–45	34	11 (7.9)	32.4	23 (9.0)	67.6
45–50	20	5 (3.6)	25.0	15 (5.9)	75.0
50–55	20	10 (7.1)	50.0	10 (3.9)	50.0
55–60	18	12 (8.6)	66.7	6 (2.4)	33.3
60–65	22	12 (8.6)	54.5	10 (3.9)	45.5
65–70	12	10 (7.1)	83.3	2 (0.8)	16.7
70–75	4	4 (2.9)	100.0	0 (0.0)	0.0
75–80	0	0 (0.0)		0 (0.0)	
80–85	28	22 (15.7)	78.6	6 (2.4)	21.4
85–90	8	8 (5.7)	100.0	0 (0.0)	0.0
90–95	16	14 (10.0)	87.5	2 (0.8)	12.5
95–100	19	8 (5.7)	42.1	11 (4.3)	57.9
Total	395	140 (35%)		255 (65%)	

terhelical modes and the modes with frequency larger than 85 cm^{-1} [14] were thought to be the intrahelical modes. This observation agrees with our result.

D. Frequency shifts of the intrahelical modes

Frequencies increase from the segment modes to the intrahelical crystal modes due to the crystal force field. The frequency shift should indicate the strength of the interhelical interactions on each particular intrahelical mode. The bigger the potential energy due to the interhelical interactions is, the larger the frequency shift becomes. We confirmed this point by using a simplified model for the potential energy due to the interhelical interactions [15].

E. Einstein absorption and extinct coefficient

The infrared absorption intensities of the DNA modes [2,16] are proportional to $|\sum_i (e_i/\sqrt{m_i})q^l_{iz}|^2/\omega$ for the longitudinal polarization and

$$\frac{1}{2}\left|\sum_i (e_i/\sqrt{m_i})(q^l_{ix}+q^l_{iy})\right|^2/\omega$$

for tranversal polarization. For antiphase crystal modes, the overall dipole moment of the crystal unit cell vanishes. Therefore they will not be detected in the observations of microwave or infrared absorption. Figure 2 is the plot for these values versus the in-phase crystal modes. The summation is taken over all of the atoms in the crystal unit cell and the Cartesian displacements of each crystal mode were normalized.

This result agrees with the selection rules derived by Higgs [17]; i.e., only the modes with $\theta_b=0$ or Φ (pitch angle of the helix) have contribution to the infrared absorption. The Raman scattering also occurs in the crystal modes with $\theta_b=2\Phi$. We therefore predict peaks in infrared absorption at 35, 50, and 83 cm^{-1}. The band with greatest absorption is at 83 cm^{-1} followed by 35 cm^{-1} and the weakest of the three is at 50 cm^{-1}.

Experimental data on far-infrared absorption in nucleic acid crystals exist for the RNA crystal poly(rI)·poly(rC), which is an RNA double helix of inosine and cytosine bases [18]. Three prominent absorption features are found centered around 32, 50, and 65 cm^{-1}. We will show that the behavior of these features has much in common with our predicted 35-, 50-, and 83-cm^{-1} absorption peaks. The experimentally observed features are very broad as expected for thermally activated modes.

F. Counterion-dependent modes

We can decompose a DNA molecule into five subunits; i.e., the sugar rings, phosphate groups, G and C bases, and the sodium ions. The motion of the center of mass of these units and the thermal motion of the atoms relative to the center of mass were discussed elsewhere [15]. In some modes, the movement of the sodium ions is far greater than that of the rest of the atoms. These modes are expected to depend significantly on the type of counterions in the DNA crystal. These modes would soften, i.e., the frequencies decrease, when the mass of the ion increases and stiffens; i.e., the frequencies increase, while the charge of the ions increases. Tables III–VI list the

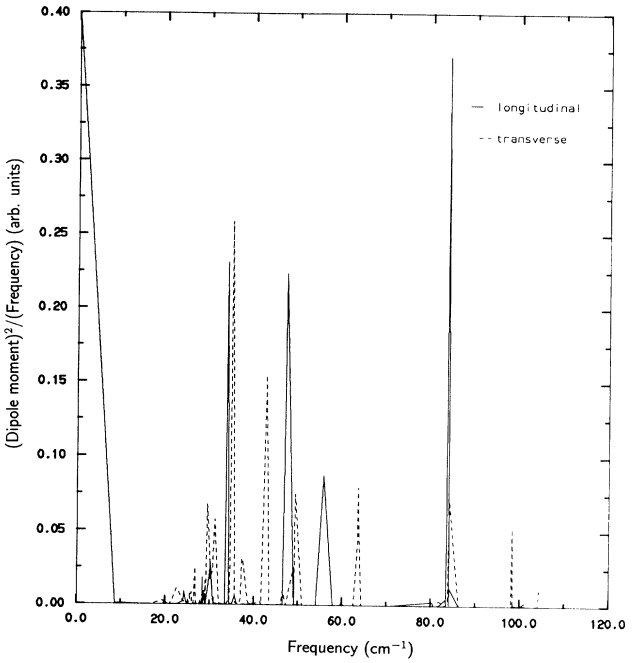

FIG. 2. Square of dipole moment/frequency vs frequency for the in-phase crystal modes. These values reflect infrared absorption intensities.

counterion-dependent modes which peak in the infrared spectrum and those which are Raman scattering sensitive.

1. Counterion-dependent modes: Infrared sensitive modes

We predicted that infrared absorption peaks at frequencies of 35, 50, and 83 cm^{-1}. In Table III there are no counterion-dependent modes with significant intensity in the frequency regions near 35 and 50 cm^{-1}. Therefore these two bands should not depend strongly on the counterion species. In the 83-cm^{-1} band, the dominant mode, i.e., the 83.817-cm^{-1} mode, is counterion dependent. Therefore we expect the 83-cm^{-1} band to depend strongly on the type of counterion. As the counterion's mass increases and the charge stays the same, the intensity of the infrared absorption for the counterion-dependent modes would decrease along with frequency decrease [15].

Compared with the experimental observations in RNA crystals [18], the features at 32 and 50 cm^{-1} do not

TABLE III. Counterion-dependent modes: the modes which peak in the infrared spectrum.

Frequency (cm^{-1})	Relative intensity	Assignment
29.416	0.18(xy)	Interhelical
63.507	0.22(xy)	Intrahelical ($\theta_b=32°$)
83.817	1.00(z)	Intrahelical ($\theta_b=0°$)
84.079	0.19(xy)	Intrahelical ($\theta_b=32°$)
84.170	0.19(xy)	Interhelical

TABLE IV. Counterion-dependent modes: the modes are mainly from the segment modes with $\theta_b = 0.0°$.

Frequency (cm^{-1})	Assignment
28.399	Interhelical
28.493	Interhelical
28.645	Interhelical
28.658	Interhelical
29.977	Interhelical
30.180	Intrahelical ($\theta_b = 0°$)
30.379	Interhelical
33.861	Intrahelical ($\theta_b = 0°$)
34.152	Intrahelical ($\theta_b = 0°$)
47.236	Intrahelical ($\theta_b = 0°$)
47.307	Intrahelical ($\theta_b = 0°$)
63.358	Intrahelical ($\theta_b = 0°$)
63.372	Intrahelical ($\theta_b = 0°$)
63.700	Intrahelical ($\theta_b = 0°$)
63.782	Intrahelical ($\theta_b = 0°$)
83.817	Intrahelical ($\theta_b = 0°$)
83.861	Intrahelical ($\theta_b = 0°$)
84.170	Interhelical
84.185	Interhelical

change significantly with counterion species but the 65-cm^{-1} feature does.

2. *Counterion-dependent modes: Raman scattering sensitive modes*

From Tables IV–VI we notice that many Raman scattering sensitive counterion-dependent modes occur at around 30 cm^{-1}. Since we have a large mode density for the Raman scattering sensitive modes around 30 cm^{-1}, we expect that there is a peak in the Raman spectrum around 30 cm^{-1} and this peak is counterion dependent. A significant experimental 25-cm^{-1} band was cited for DNA crystals at 75% relative humidity and it was predicted to be at 30 cm^{-1} at 0% relative humidity by using a mass-loading model [19]. The frequency shift of this band with counterion species agrees with what we predict for the counterion-dependent modes.

TABLE V. Counterion-dependent modes: the modes are mainly from the segment modes with $\theta_b = 32°$.

Frequency (cm^{-1})	Assignment
29.416	Interhelical
30.806	Interhelical
30.847	Interhelical
30.938	Interhelical
30.952	Interhelical
31.025	Interhelical
31.050	Interhelical
63.507	Intrahelical mode ($\theta_b = 32°$)
63.565	Intrahelical mode ($\theta_b = 32°$)
84.034	Intrahelical mode ($\theta_b = 32°$)
84.079	Intrahelical mode ($\theta_b = 32°$)

TABLE VI. Counterion-dependent modes: the modes are mainly from the segment modes with $\theta_b = 65°$.

Frequency (cm^{-1})	Assignment
28.360	Interhelical
29.022	Interhelical
29.025	Interhelical
30.698	Interhelical
30.721	Interhelical
49.117	Intrahelical ($\theta_b = 65°$)
62.491	Intrahelical ($\theta_b = 65°$)
62.493	Intrahelical ($\theta_b = 65°$)
62.554	Interhelical
62.555	Interhelical
83.409	Intrahelical ($\theta_b = 65°$)
83.417	Intrahelical ($\theta_b = 65°$)
83.436	Intrahelical ($\theta_b = 65°$)
83.447	Intrahelical ($\theta_b = 65°$)

G. Observed 25- and 35-cm^{-1} modes in Raman scattering spectrum

The Raman scattering spectrum is the result of summing all of the peaks for the sensitive modes. We predict that the frequency region where large mode density (number of modes per wave number) for the Raman scattering sensitive modes occurs is where the Raman spectrum peaks. This frequency range is from 20 to 40 cm^{-1}.

There are two bands sited at 25 and 35 cm^{-1} in the Raman spectrum of the DNA crystal with sodium ions at 75 relative humidity [19–21]. With the mass-loading model for the water molecules, they are predicted to be the 30- and 46-cm^{-1} modes at 0 relative humidity [20] where mass loading is absent. Both bands show large Raman scattering intensity in *VH* and *HV* polarization. The 46-cm^{-1} mode has weaker scattering in the polarized spectra (*VV* and *VH*). The selection rules tell us that both bands consist of crystal modes which are mainly from the segment modes $\theta_b = \Phi$ and the 46-cm^{-1} band also has the crystal modes with $\theta_b = 0$. The characteristics of these two bands agree with our results. Since there are no intrahelical modes in the range 20–30 cm^{-1}, the 30-cm^{-1} band should show characteristics of an interhelical band. As to the 46-cm^{-1} band, we found two intrahelical modes which belong to group $\theta_b = \Phi$; i.e., 42.634 cm^{-1} in-phase and 42.654 cm^{-1} antiphase modes. This explains why this band also appeared in the spectrum of DNA in solution.

V. CONCLUSIONS

The interhelical interactions associated with the crystalline packing of individual helices are found to have two effects on the modes of separated individual helices. The first effect can be described as a crystal field shift in frequency. The second effect is a mixing of isolated helix modes into new crystal modes. This latter group of modes are the interhelical modes which do not occur in the isolated helices. 35% of the crystal modes in our restricted frequency range were found to be intrahelical modes and 65% interhelical modes. 53% of these crystal

modes fall in the frequency range 20–45 cm^{-1}. 64% of the interhelical modes fall in the 20–45-cm^{-1} region with 20–25 cm^{-1} being the area where the interhelical mode density is the largest. The intrahelical modes spread out in the range considered and, generally speaking, there are more intrahelical modes in the high-frequency regions than there are in low-frequency regions. The interhelical modes dominate in the frequency range 25–30 cm^{-1}. The intrahelical modes dominate in the region with frequency greater than 80 cm^{-1}. The frequency shifts of the intrahelical modes from the segment modes were expected to be strongly associated with the increase of the force field due to the interhelical interactions. This point was confirmed through the use of a simplified model for the potential energy due to the interhelical interactions. For modes above 100 cm^{-1} we expect mostly intrahelical modes.

The selection rules for an isolated DNA double helix can be applied to the DNA crystal with the exception that the antiphase crystal modes are not infrared sensitive. The selection rules state that infrared absorption occurs at the helix modes with phase difference between base pairs, θ_b, equal to 0 or Φ, whereas Raman scattering occurs also at the helix modes with $\theta_b = 2\Phi$. The infrared absorption for the crystal was found to peak at 35, 50, and 83 cm^{-1}. Intensity of Raman scattering is closely associated with polarizability of the DNA crystal which can only be calculated theoretically by determining the electronic band structure. Therefore we are not able to predict the spectrum of Raman scattering except the location of the Raman scattering sensitive modes. However, we suspect that Raman scattering peaks at around 30 cm^{-1} where the density of the Raman scattering sensitive modes is the largest. A major Raman scattering band was cited at around 25 cm^{-1} in experimental observations. The characteristics of this band along with that of the other observed band at 35 cm^{-1} agree with what was predicted.

Those crystal modes where the motion falls mainly on the counterions are expected to depend strongly on the particular counterions. The 35- and 50-cm^{-1} infrared absorption bands do not have large counterion motion and should therefore have no great dependence on ion species. This prediction is in rough agreement with the observed 30- and 50-cm^{-1} features in RNA crystals. The 83-cm^{-1} band has much ion motion and should be strongly dependent on the counterion as is the case for the experimentally observed 65-cm^{-1} feature in RNA crystals.

In conclusion we do find rough agreement between our predictions and experimental observations in the 20–35-cm^{-1} region. This includes frequencies and salt dependence. The RNA features at ≈ 65 cm^{-1} seem to be associated with our DNA predicted peak at 83 cm^{-1}. The difference may be due to water hydration effects not included in our model.

ACKNOWLEDGMENT

This work was supported in part by ONR Contract No. N00014-92-K-1232.

APPENDIX A: DNA MOLECULE WITH ONE 360° TURN AS A UNIT CELL

Since the DNA crystal unit cell consists of 360° DNA turns, we need the normal modes of an isolated DNA molecule with a 360° turn as a unit cell to calculate the normal modes of the DNA crystal through the Green-function method. The dynamics of the DNA molecule with a 360° turn, "a segment," as a repetitive unit cell can be derived from that of a DNA molecule with a single base pair as a unit cell.

The equation of motion for a DNA molecule with a segment as a unit is

$$[M_s(\theta_s)S_s(\theta_s)-S_s(\theta_s)\Lambda_s(\theta_s)]=0 \ . \tag{A1}$$

θ_s is the phase difference between consecutive segments.

For a one-dimensional lattice, the wave vector k at the first Brillouin zone lies in the range $-\pi/d < k < \pi/d$ with d being the size of a unit cell. Let a be the cell size of one base-pair lattice. The first Brillouin zone for a DNA molecule with one base pair as a unit cell is $-\pi/a < k_b < \pi/a$ and for the DNA molecule with one segment as a unit is $-\pi/11a < k_s < \pi/11a$. The dispersion curve of the DNA molecule with one segment as a unit at the first Brillouin zone can be generated by folding the curve of the DNA molecule with one base pair as a unit at the first Brillouin zone. For each k_s, there are 11 corresponding k_b,

$$k_b = k_s, k_s \pm \frac{2\pi}{11a}, k_s \pm \frac{4\pi}{11a}, \ldots, k_s \pm \frac{10\pi}{11a} \ . \tag{A2}$$

The phase difference is equal to the wave number times the size of the unit cell, $\theta = ka$. For each phase difference of the DNA molecule with one segment as a unit, θ_s, we have 11 corresponding phase differences of the DNA molecule with one base pair as a unit, θ_b,

$$\theta_b = \frac{\theta_s}{11}, \frac{\theta_s \pm 2\pi}{11}, \frac{\theta_s \pm 4\pi}{11}, \ldots, \frac{\theta_s \pm 10\pi}{11} \ . \tag{A3}$$

$S_s(\theta_s)$ and $\Lambda(\theta_s)$ can be expressed in terms of $S_b(\theta_b)$ and $\Lambda(\theta_s)$, with θ_b equal to the 11 values listed above.

We label DNA base pairs as in Fig. 3. ξ_n is the MWC coordinates of the nth base pair. Let $x_0(\theta)$ be the MWC symmetry coordinates of the 0th base pair and we have

$$\begin{aligned}
\xi_0 &= \frac{1}{\sqrt{2\pi}} \int_{-\pi}^{\pi} x_0(\theta) d\theta \ , \\
\xi_1 &= \frac{1}{\sqrt{2\pi}} \int_{-\pi}^{\pi} (e^{-i\theta} R) x_0(\theta) d\theta \ , \\
\xi_2 &= \frac{1}{\sqrt{2\pi}} \int_{-\pi}^{\pi} (e^{-i\theta} R)^2 x_0(\theta) d\theta \ , \\
&\vdots \\
\xi_n &= \frac{1}{\sqrt{2\pi}} \int_{-\pi}^{\pi} (e^{-i\theta} R)^n x_0(\theta) d\theta \ .
\end{aligned} \tag{A4}$$

Let Ξ be the MWC coordinates of the segment unit cell, which includes base pair 0 to 10. We have

$$\Xi=\begin{bmatrix}\xi_0\\ \xi_1\\ \xi_2\\ \vdots\\ \xi_{10}\end{bmatrix}=\frac{1}{\sqrt{2\pi}}\int_{-\pi}^{\pi}\begin{bmatrix}x_0(\theta)\\ (e^{-i\theta}R)x_0(\theta)\\ (e^{-i\theta}R)^2x_0(\theta)\\ \vdots\\ (e^{-i\theta}R)^{10}x_0(\theta)\end{bmatrix}d\theta\ . \tag{A5}$$

Since each θ_s leads to 11 corresponding θ_b, we have

$$S_s(\theta_s)=\frac{1}{\sqrt{11}}\begin{bmatrix} S_b(\theta_0) & S_b(\theta_1) & \cdots & S_b(\theta_{10}\\ e^{-i\theta_0}RS_b(\theta_0) & e^{-i\theta_1}RS_b(\theta_1) & \cdots & e^{-i\theta_{10}}RS_b(\theta_{10})\\ e^{-i2\theta_0}R^2S_b(\theta_0) & e^{-i2\theta_1}R^2S_b(\theta_1) & \cdots & e^{-i2\theta_{10}}R^2S_b(\theta_{10})\\ \vdots & \vdots & \ddots & \vdots\\ e^{-i10\theta_0}R^{10}S_b(\theta_0) & e^{-i10\theta_1}R^{10}S_b(\theta_1) & \cdots & e^{-i10\theta_{10}}R^{10}S_b(\theta_{10})\end{bmatrix}, \tag{A6}$$

where $\theta_0=\theta_s/11$, $\theta_1=(\theta_s+2\pi)/11$, $\theta_2=(\theta_s+4\pi)/11,\ldots,$ $\theta_5=(\theta_s+10\pi)/11$, $\theta_6=(\theta_s-2\pi)/11$, $\theta_7=(\theta_s-4\pi)/11,\ldots,$ and $\theta_{10}=(\theta_s-10\pi)/11$. The $1/\sqrt{11}$ factor on the right-hand side is the normalization factor. If $\theta_s=0$, the 11 corresponding θ_b are 0, $-2\pi/11$, $-4\pi/11$, $-6\pi/11$, $-8\pi/11$, $-10\pi/11$, $2\pi/11$, $4\pi/11$, $6\pi/11$, $8\pi/11$, and $10\pi/11$.

The eigenvalue matrices of A-DNA with one segment as a unit, $\Lambda_s(\theta_s)$, and that of A-DNA with one base pair as a unit, $\Lambda_b(\theta_b)$, are related as follows:

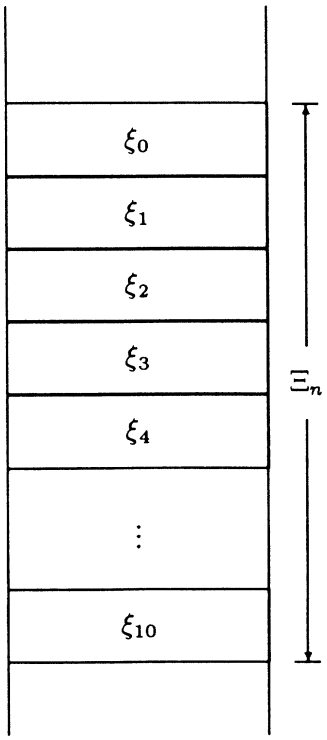

FIG. 3. Numbering of DNA base pairs. ξ_n is the unit cell of a double helix with one base pair as a unit and Ξ_n is the unit cell of a double helix with 11 base pairs as a unit.

$$\Lambda_s(\theta_s)=\begin{bmatrix}\Lambda_b(\theta_0) & 0 & 0 & \cdots & 0\\ 0 & \Lambda_b(\theta_1) & 0 & \cdots & 0\\ 0 & 0 & \Lambda_b(\theta_2) & \cdots & 0\\ 0 & 0 & 0 & \cdots & \Lambda_b(\theta_{10})\end{bmatrix}. \tag{A7}$$

The modes of a homopolymer segment can then be determined from the calculations of a system with a much smaller number of degrees of freedom i.e., the system of one base-pair unit cell. The matrix to be diagonalized is smaller by a factor of 11.

If S_b satisfies the unitary condition, $S_b^{\dagger}(\theta_b)S_b(\theta_b)=I$, so will S_s,

$$S_s^{\dagger}(\theta_s)S_s(\theta_s)=I\ . \tag{A8}$$

APPENDIX B: INTERHELICAL INTERACTION

To calculate the interhelical interactions between POOI atoms, the following equations are used for the

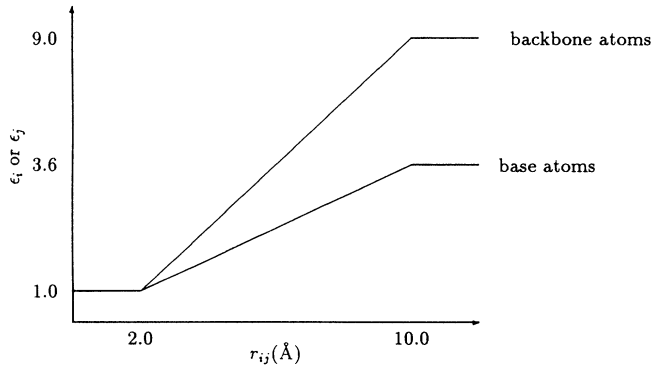

FIG. 4. Dielectric constant vs the atom separation. For atom separation less than 2.0 Å, the dielectric constant is taken as 1.0. For atom separation greater than 10.0 Å, the dielectric constant is taken as 3.6 and 9.0 for base and backbone atoms, respectively.

TABLE VII. Net charges of *A*-GC homopolymer base pair with Na^+ (guanine nucleotide).

Atom	Charge
Deoxyribose phosphate unit	
c3+H	0.2953
c4+H	0.2117
o4	−0.4855
c1+H	0.3490
c2+2H	−0.0707
o3	−0.7635
c5+2H	0.2371
o5	−0.6746
p	1.8099
o1	−0.8875
o2	−0.8911
Na^+	1.000
Guanine base unit	
n9	−0.0752
c8+H	0.1661
n7	−0.1177
c5	−0.2363
c6	0.6501
n1+H	−0.1701
c2	0.3943
n3	−0.3385
c4	0.2198
o6	−0.6128
n2+2H	−0.0097

TABLE VIII. Net charges of *A*-GC homopolymer base pair with Na^+ (cytosine nucleotide).

Atom	Charge
Deoxyribose phosphate unit	
c3+H	0.2938
c4+H	0.2133
o4	−0.4860
c1+H	0.3897
c2+2H	−0.0886
o3	−0.7598
c5+2H	0.2365
o5	−0.6790
p	1.8107
o1	−0.8857
o2	−0.8962
Na^+	1.000
Cytosine base unit	
n1	−0.1862
c6+H	0.2558
c5+H	−0.2667
c4	0.3907
n3	−0.4496
c2	0.6823
o2	−0.6313
n4+2H	−0.0563

force constants of the nonbonded interaction between atoms i and j [2,12]:

$$f_{ij}=f_1+f_2 , \tag{B1}$$

$$f_1=2\eta\frac{|e_ie_j|}{\sqrt{\epsilon_i\epsilon_j}r_{ij}^3} , \tag{B2}$$

$$f_2=42\frac{A}{r_{ij}^8} . \tag{B3}$$

f_1 is for the electrostatic interaction and f_2 the van der Waals interaction. r_{ij} is the distance between the atoms. e_i and e_j are the unbalanced charges in units of electron charge. ϵ_i and ϵ_j are the dielectric constants pertinent to atoms i and j. Constants η and A were chosen to be 0.43 and 0.12 [2,22].

The electrostatic terms require both a charge distribution, i.e., the net charge on each atom, and a choice of effective dielectric constant between these atoms. When the atoms are neighbors, no dielectric matter is between them and the effective dielectric constant should be one. When the atoms are far away and much matter is between them, the bulk dielectric constant is appropriate. We use a functional form for the dielectric constant that contains these two limiting values and linearly extrapolate the value between them [23,24]. A plot of this function form is shown in Fig. 4. The bulk values depend on the material. Net charges of the atoms of *A*-GC homopolymer are listed in Tables VII and VIII.

[1] J. M. Eyster and E. W. Prohofsky, Biopolymers **13**, 2505 (1974).

[2] B. L. Young, V. V. Prabhu, and E. W. Prohofsky, Phys. Rev. A **39**, 3173 (1989).

[3] K. C. Lu, E. W. Prohofsky, and L. L. Van Zandt, Biopolymers **16**, 2491 (1977).

[4] S. M. Lindsay, in *Proceedings of the International Symposium on Computer Analysis for Life Science,* edited by C. Kawabata and A. R. Bishop (Ohmsha, Tokyo, 1986), pp. 89–98.

[5] R. Chandrasekaran, M. Wang, R.-G. He, L. C. Puigjaner, M. A. Byler, R. P. Millane, and Struther Arnott, J. Biomol. Struct. Dynamics **6**, 1189 (1989).

[6] E. Clementi and G. Corongiu, IBM DPPG Research Report No. POK-1, 1981 (unpublished).

[7] E. Clementi, in *Structure and Dynamics: Nucleic Acids and Proteins,* edited by E. Clementi and R. H. Sarma (Adenine, New York, 1983), pp. 321–364.

[8] V. V. Prabhu, Ph.D. thesis, Purdue University, 1988 (unpublished).

[9] K. M. Awati, Ph.D. thesis, Purdue University, 1989 (unpublished).

[10] J. M. Eyster and E. W. Prohofsky, Biopolymers **16**, 965 (1977).

[11] E. B. Wilson, Jr., J. C. Decius, and P. C. Cross, *Molecular Vibrations: The Theory of Infrared and Raman Vibrational Spectra* (McGraw-Hill, New York, 1955).

[12] J. M. Eyster and E. W. Prohofsky, Biopolymers **13**, 2527 (1974).

[13] S. M. Lindsay and J. Powell, in *Structure and Dynamics: Nucleic Acids and Proteins,* edited by E. Clementi and R. H. Sarma (Adenine, New York, 1983), pp. 241–259.

[14] T. Weidlich (private communication).
[15] L. Chern, Ph.D. thesis, Purdue University, 1992 (unpublished).
[16] M. Kohli, W. N. Mei, E. W. Prohofsky, and L. L. Van Zandt, Biopolymers **20**, 853 (1981).
[17] P. W. Higgs, Proc. R. Soc. London, Ser. A **220**, 472 (1953).
[18] T. Weidlich, Biopolymers **30**, 477 (1990).
[19] T. Weidlich, Ph.D. thesis, Arizona State University, 1989 (unpublished).
[20] S. M. Lindsay, S. A. Lee, J. W. Powell, R. Weidlich, C. DeMarco, G. D. Lewen, and N. J. Tao, Biopolymers **27**, 1015 (1988).
[21] T. Weidlich, S. M. Lindsay, S. A. Lee, N. J. Tao, G. D. Lewen, W. L. Peticolas, G. A. Thomas, and A. Rupprecht, J. Phys. Chem. **92**, 3315 (1988).
[22] D. A. Pearlman and S. H. Kim, Biopolymers **24**, 327 (1985).
[23] L. Young, V. V. Prabhu, and E. W. Prohofsky, Phys. Rev. A **39**, 3173 (1989).
[24] K. S. Girrirajan, L. Young, and E. W. Prohofsky, Biopolymers **28**, 1841 (1989).